
An efficient algorithm for numerical homogenization of fluid filled porous solids: part-I

Saumik Dana
University of Southern California
Los Angeles, CA 90007
sdana@usc.edu

Mary F Wheeler
Oden Institute for Computational Engineering and Sciences
University of Texas at Austin
Austin, TX 78712

ABSTRACT

The concept of representative volume element or RVE is invoked to develop an algorithm for numerical homogenization of fluid filled porous solids. RVE based methods decouple analysis of a composite material into analyses at the local and global levels. The local level analysis models the microstructural details to determine effective properties by applying boundary conditions to the RVE and solving the resultant boundary value problem. The composite structure is then replaced by an equivalent homogeneous material having the calculated effective properties. We combine the features of two techniques: one is the definition of a displacement field for the fluid phase to allow for a definition of a continuous displacement field across the microstructure and the other is the FE^2 numerical homogenization that couples the macroscale with the RVE scale via gauss points.

Keywords RVE · Homogenization · Fluid-structure interaction · Algorithm

1 Introduction

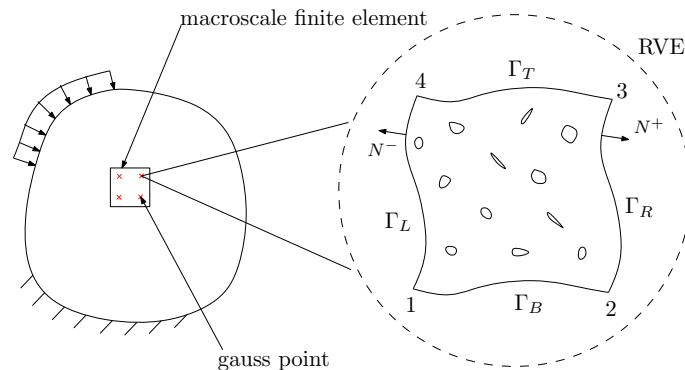


Figure 1: A 2D depiction of the algorithmic framework. The macroscale boundary value problem is discretized into finite elements. The gauss point level computations for the macroscale BVP work in conjunction with RVE scale solve corresponding to each gauss point.

The RVE concept [1–8] is commonly used in the aerospace/automotive industry to avoid using computationally expensive simulation platforms necessary to capture microstructural features. In essence, the features are captured in the RVE and averaged out over the RVE before any discretization technique is employed at the macroscale with the averaged properties as parameters. More often than not, a number of simulations are run with different microstructures and the statistical mean of the results from those simulations on the

macroscale are used as guiding principles for the design of the aerospace/automotive part. The reason for running multiple simulations each with a different microstructure is that the microstructure is only known stochastically and not deterministically. With advances in the field of material science and increased emphasis on modeling of biological tissues and engineered structures like foams and textiles, the need is felt to extend the analyses for cases in which both solid and fluid phases exist in tandem in the microstructure. The problem is complicated since the physics of solid dictates focus on solid displacements while the physics of fluid dictates focus on fluid velocities. The displacements and velocities are dimensionally incompatible since the velocity represents the rate of change of fluid displacement. In lieu of that, we employ the technique in which a displacement field is defined for the fluid phase also to go with the displacement field defined naturally for the solid phase [9]. We combine that technique with the FE^2 homogenization framework [10–12] in which each gauss point for the finite element calculations at the macroscale is associated with a RVE and the information exchange between the two scales occurs at each of those gauss points via the deformation gradient. A 2D depiction of the algorithmic framework is given in Figure 1. The reason for calling the framework FE^2 is that both the macroscale and the RVE scale are solved using finite element method. The accuracy of the RVE approximation depends on how well the assumed boundary conditions reflect each of the myriad boundary conditions to which the RVE is subjected in-situ. The imposed boundary conditions on the RVE should be such that the Hill-Mandel condition [3, 13–20] of energetic equivalence between the two scales is satisfied. Periodic boundary conditions satisfy the Hill-Mandel condition and are generally the optimal choice from the standpoint of macroscale accuracy [21–34]. It is important to note that this framework is meant for monolithic solution of the coupled system of equations as opposed to the popular fixed stress split strategy [35–42] in which the coupled set of equations are first decoupled and then solved sequentially and iteratively until convergence at each time step. This paper is structured as follows: we explain the concepts of deformation gradient and first P-K stress in this Section. We present the algorithmic framework for numerical homogenization in purely mechanical case in Section 2. We then proceed to present the algorithmic framework in the hydromechanical case of fluid filled porous solids in Section 3. We finally present conclusions and outlook in Section 4. An important part of the derivation of the RVE level system of equations for the fluid filled porous solid case will be dealt with in part-II of this paper.

1.1 The deformation gradient and first P-K stress

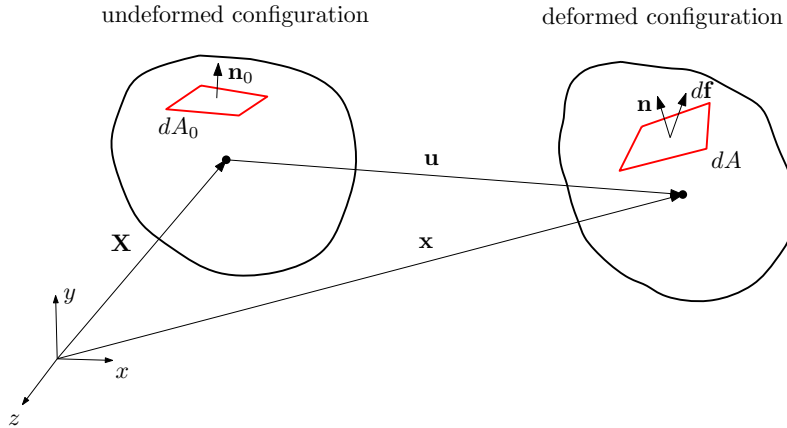


Figure 2: \mathbf{X} is position vector of point in reference configuration and $\mathbf{x} = \mathbf{X} + \mathbf{u}$ is the position vector the same point in the deformed configuration. Meanwhile, an elemental area dA_0 with unit normal \mathbf{n}_0 deforms to dA with unit normal \mathbf{n} under the transformation.

As shown in Figure 2, let \mathbf{u} be the macroscale deformation field. The macroscale deformation gradient \mathbf{F}_M is the macroscale spatial derivative of \mathbf{x} in the reference configuration as follows

$$\mathbf{F} = \mathbf{x} \otimes \nabla_{\mathbf{X}} \equiv \mathbf{I} + \mathbf{u} \otimes \nabla_{\mathbf{X}}$$

An incremental force $d\mathbf{f}$ is defined with respect to the Cauchy stress $\boldsymbol{\sigma}$ and the first Piola-Kirchhoff stress \mathbf{P} in the deformed and reference configurations respectively as follows

$$d\mathbf{f} = \boldsymbol{\sigma} \mathbf{n} dA = \mathbf{P} \mathbf{n}_0 dA_0$$

2 Algorithmic framework for the pure mechanical case

In the initialization stage,

- ✓ The macroscale deformation gradient is set to identity tensor since that would imply the macroscale BVP starts at the reference configuration
- ✓ The macroscale BVP is discretized into finite elements and an RVE is assigned to each gauss point
- ✓ The macroscale tangent stiffness is not known apriori and is obtained at each gauss point from RVE level computations as shown in module 2.2

Once the initialization phase is complete,

1. An increment of macro load is applied
2. Macroscale BVP is solved
3. The macroscale deformation gradient is updated
4. Periodic boundary conditions are imposed on RVE in accordance with (1)
5. RVE BVP is solved and homogenized first P-K stress is obtained in accordance with (6)
6. The gauss point level homogenized first P-K stress is used to compute internal forces at macroscale finite element nodes

If these internal forces are in balance with the prescribed macro load, incremental convergence has been achieved and steps 1 – 6 are repeated. If that is not the case, steps 2 – 6 are repeated.

2.1 Periodic boundary conditions on RVE

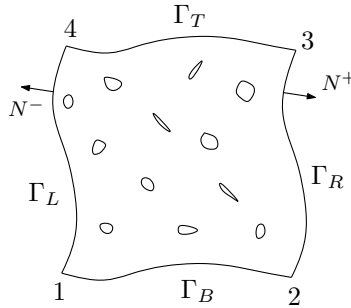


Figure 3: Typical 2D RVE with pertinent microstructural features. Γ_L and Γ_R are mirror images so are Γ_T and Γ_B . This helps in easy implementation of periodic boundary conditions on the RVE in accordance with [24].

The typical RVE for imposition of periodic boundary conditions is shown in Figure 3. After each macroscale BVP solve, the deformation gradient is updated and the new position vectors of the vertices of the RVE are obtained using

$$\mathbf{x} = \mathbf{F}_M \mathbf{X} \quad (1)$$

where \mathbf{X} represents position vector in the reference configuration. This alongwith the shape periodicity of the RVE enables the implementation of periodic boundary conditions on RVE. It is easy to see that the prescribed periodic boundary conditions are Dirichlet boundary conditions.

2.2 Computation of homogenized tangent stiffness at the macroscale

The linear momentum balance for the macroscale BVP in the reference configuration is given by

$$\nabla_{\mathbf{X}} \cdot \mathbf{P}_M + \mathbf{b} = \mathbf{0}$$

where \mathbf{b} is the body force vector. The macroscale incremental constitutive law is

$$\delta \mathbf{P}_M = \mathbb{C}_M \delta \mathbf{F}_M \quad (2)$$

where \mathbb{C}_M is the fourth order macroscale material property tensor. The determination of \mathbb{C}_M proceeds as follows: First, the RVE scale linear momentum balance is expressed in the indicial notation as

$$P_{ik,k} + b_i = 0 \quad i, k = 1, 2, 3$$

where the notation $(\cdot)_{,k}$ is used to denote the spatial derivative in the reference configuration as follows

$$(\cdot)_{,k} \equiv \frac{\partial(\cdot)}{\partial X_k}$$

Before we proceed, we assume that the body force is zero, and obtain the following using chain rule for differentiation

$$(P_{ik} X_j)_{,k} = P_{ik,k} X_j + P_{ik} \delta_{jk} = -b_i X_j + P_{ij} \quad (3)$$

We express the macroscale first P-K stress in indicial notation as follows

$$P_{Mij} = \frac{1}{V_0} \int_{V_0} P_{ij} dV_0 = \frac{1}{V_0} \int_{V_0} (P_{ik} X_j)_{,k} dV_0 = \frac{1}{V_0} \int_{\Gamma_0} P_{ik} n_{0k} X_j d\Gamma_0 \quad (4)$$

where the third equality follows from (3) and the fourth equality follows from divergence theorem. We then write (4) in tensorial notation as

$$\mathbf{P}_M = \frac{1}{V_0} \int_{\Gamma_0} \mathbf{t}_0 \otimes \mathbf{X} d\Gamma_0 \quad (5)$$

We know that the RVE level BVP is also solved using finite elements. Let N_p be the number of boundary nodes for the RVE scale discretized domain and let $\mathbf{f}_p^{(i)}$ be the force on i^{th} boundary node. We can rewrite (5) as

$$\mathbf{P}_M = \frac{1}{V_0} \int_{\Gamma_0} \mathbf{t}_0 \otimes \mathbf{X} d\Gamma_0 = \frac{1}{V_0} \sum_{i=1}^{N_p} \mathbf{f}_p^{(i)} \otimes \mathbf{X}^{(i)} \quad (6)$$

It is important to note that these boundary forces are not known apriori and are obtained from the RVE level solve. Let \mathbf{u}_f represent the displacement DOFs corresponding to the interior nodes and \mathbf{u}_p represent the displacement DOFs corresponding to the boundary nodes. The force displacement relation for the RVE scale problem is

$$\overbrace{\begin{bmatrix} \mathbf{K}_{pp} & \mathbf{K}_{pf} \\ \mathbf{K}_{fp} & \mathbf{K}_{ff} \end{bmatrix}}^{\mathbf{K}^{RVE}} \begin{Bmatrix} \delta \mathbf{u}_p \\ \delta \mathbf{u}_f \end{Bmatrix} = \begin{Bmatrix} \delta \mathbf{f}_p \\ \mathbf{0} \end{Bmatrix}$$

where the matrix \mathbf{K}^{RVE} is dictated by the microstructure and is known apriori. We knock off DOFs corresponding to internal nodes to obtain

$$\overbrace{\begin{bmatrix} \mathbf{K}_{pp} - \mathbf{K}_{pf}(\mathbf{K}_{ff})^{-1}\mathbf{K}_{fp} \end{bmatrix}}^{\mathbf{K}} \{\delta \mathbf{u}_p\} = \{\delta \mathbf{f}_p\} \quad (7)$$

The incremental macroscopic first PK stress is obtained as

$$\delta \mathbf{P}_M = \frac{1}{V_0} \sum_{i=1}^{N_p} \delta \mathbf{f}_p^{(i)} \otimes \mathbf{X}^{(i)} \quad (\text{from (6)})$$

$$\begin{aligned}
 &= \frac{1}{V_0} \sum_{i=1}^{N_p} \sum_{j=1}^{N_p} \mathbf{K}^{(ij)} \delta \mathbf{u}_p^{(j)} \otimes \mathbf{X}^{(i)} \quad (\text{from (7)}) \\
 &= \frac{1}{V_0} \sum_{i=1}^{N_p} \sum_{j=1}^{N_p} \mathbf{K}^{(ij)} \delta \mathbf{F}_M \mathbf{X}^{(j)} \otimes \mathbf{X}^{(i)} \quad (\delta \mathbf{u} = \delta \mathbf{F}_M \mathbf{X}) \quad (8)
 \end{aligned}$$

Comparing (8) with (2), we get

$$\mathbb{C}_{M_{abcd}} = \frac{1}{V_0} \sum_{i=1}^{N_p} \sum_{j=1}^{N_p} \mathbf{K}_{ac}^{(ij)} \mathbf{X}_b^{(i)} \mathbf{X}_d^{(j)} \quad a, b, c, d = 1, 2, 3 \quad (9)$$

Algorithm 1 Pure mechanical case

```

FM ← I                                     ▷ Initialize deformation gradient
for E ∈  $\mathcal{T}_h$  do                             ▷ loop over macroscale finite elements
  for g ∈  $\mathcal{G}$  do                                 ▷ loop over gauss points
    RVE ↔ g                                       ▷ Assign a RVE to each gauss point
    Discretize the RVE
    Calculate homogenized macroscopic tangent stiffness in accordance with (9) and store it
    Assemble macroscopic tangent stiffness over gauss points
  Assemble macroscopic tangent stiffness over finite elements
while t ≤ T do
  Apply increment of macro load
  while (Internal force-Macro load > TOL) do
    Solve macroscale problem for  $\delta \mathbf{F}_M$ 
    FM ← FM +  $\delta \mathbf{F}_M$                                ▷ Update deformation gradient
    for E ∈  $\mathcal{T}_h$  do                             ▷ loop over macroscale finite elements
      for g ∈  $\mathcal{G}$  do                             ▷ loop over gauss points
        Prescribe periodic BCs in accordance with (1)
        Solve RVE problem
        Calculate first P-K stress in accordance with (6)
      Compute internal forces at finite element nodes
  
```

3 Algorithmic framework for fluid filled porous solid case

In accordance with [9] and as shown in Figure 4, the solid phase inside the RVE is located in Ω_s and the fluid phase is located in Ω_f . The interface between the two phases is Γ_{int} . A fictitious elastic material is introduced in Ω_f . The material is then attached to the internal boundary Γ_{int} . As the interface moves, the fictitious elastic material is deformed, and the nodes inside Ω_f follow the deformation of the solid. Let $\Gamma = \Gamma_f \cup \Gamma_s$ where Γ_f is the part of Ω_f where fluid can enter or exit the domain and Γ_s is the part of Ω_s on the outer boundary.

3.1 Variables involved

- ✓ RVE scale displacement field $\mathbf{u} = \left\{ \begin{array}{l} \mathbf{u}_s \text{ in } \Omega_s, \\ \mathbf{u}_f \text{ in } \Omega_f, \end{array} \right\}$
- ✓ RVE scale first P-K stress $\mathbf{P} = \left\{ \begin{array}{l} \mathbf{P}^s \text{ in } \Omega_s, \\ \mathbf{P}^f \text{ in } \Omega_f, \end{array} \right\}$
- ✓ Macroscale displacement field $\tilde{\mathbf{u}}$
- ✓ Macroscale pressure field \tilde{p}

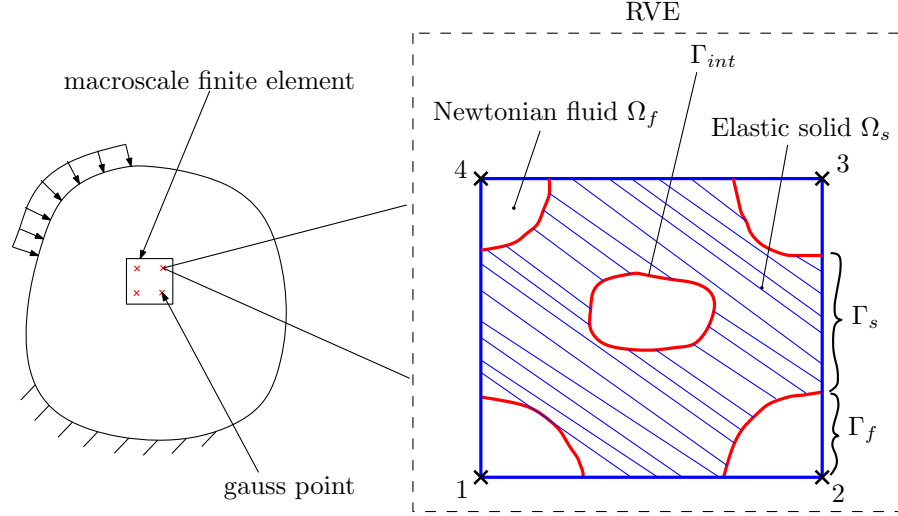


Figure 4: A 2D depiction of the algorithmic framework. The macroscale boundary value problem is discretized into finite elements. The gauss point level computations for the macroscale BVP work in conjunction with RVE scale solve corresponding to each gauss point. Many pore morphology possibilities exist and we consider only one of those possibilities here.

- ✓ RVE scale fluid pressure field p in Ω_f
- ✓ RVE scale fluid velocity field \mathbf{v} in Ω_f
- ✓ RVE scale relative fluid-solid velocity field $\mathbf{w} \equiv \mathbf{v} - \frac{d\mathbf{u}_f}{dt}$ on Γ_{int}

3.2 RVE level equations

In accordance with [9], the analysis is restricted to that of laminar and incompressible flow without convective acceleration i.e. Stokes' flow. Let $\mathbf{F} = \mathbf{I} + \mathbf{u}_f \otimes \nabla_X$ be the deformation gradient of the fictitious elastic material and let $J = \det \mathbf{F}$. The fluid-structure interaction problem in the reference configuration is

$$\left. \begin{aligned} \nabla \cdot \mathbf{P}^s &= 0 \text{ in } \Omega_s && \text{(linear momentum balance of solid phase)} \\ \nabla \cdot \mathbf{P}^f &= 0 \text{ in } \Omega_f && \text{(linear momentum balance of fictitious solid)} \\ J\mathbf{F}^{-T} : [\mathbf{v} \otimes \nabla] &= 0 \text{ in } \Omega_f && \text{(mass conservation of fluid phase)} \end{aligned} \right\}$$

On the internal boundary Γ_{int} , we have

- ✓ $\mathbf{P}_s \mathbf{n} + \mathbf{P}_f \mathbf{n} = \mathbf{0}$
- ✓ $\mathbf{u}_f = \mathbf{u}_s$
- ✓ $\mathbf{w} = \mathbf{0}$

3.3 Periodic boundary conditions on RVE

Let \mathbf{X}_c be position vector of center point of RVE in reference configuration, $\tilde{p}|_c$ be macroscale pressure field evaluated at \mathbf{X}_c and $(\nabla_X \tilde{p})|_c$ be the macroscale spatial gradient of \tilde{p} evaluated at \mathbf{X}_c . The periodic boundary conditions are

- ✓ $\mathbf{x} = \mathbf{F}_M \mathbf{X} = (\mathbf{I} + \nabla_X \tilde{\mathbf{u}}) \mathbf{X} \quad \forall \text{ RVE vertices}$
- ✓ $p = \tilde{p}|_c + (\nabla_X \tilde{p})|_c \cdot (\mathbf{X} - \mathbf{X}_c), \quad \forall \text{ RVE vertices}$

3.4 Computation of homogenized macroscopic tangent stiffness and first P-K stress

The RVE level system of equations is obtained as

$$\begin{bmatrix} \mathbf{K}_{uu} & \mathbf{K}_{up} \\ \mathbf{K}_{pu} & \mathbf{K}_{pp} \end{bmatrix} \begin{Bmatrix} \delta \mathbf{u} \\ \delta p \end{Bmatrix} = \begin{Bmatrix} \delta \mathbf{f}_s \\ \delta \mathbf{f}_p \end{Bmatrix} \quad (10)$$

where \mathbf{f}_s and \mathbf{f}_p are resulting boundary forces corresponding to the solid and fluid phases respectively. The details of the derivation of (10) will be explained in part-II of this paper. The incremental macroscopic first PK stresses are obtained as

$$\begin{Bmatrix} \delta \mathbf{P}_{sM} \\ \delta \mathbf{P}_{fM} \end{Bmatrix} = \begin{Bmatrix} \frac{1}{|\Omega_s|} \int_{\Omega_s} \delta \mathbf{P}_s \\ \frac{1}{|\Omega_f|} \int_{\Omega_f} \delta \mathbf{P}_f \end{Bmatrix} = \begin{Bmatrix} \frac{1}{|\Omega_s|} \int_{\Gamma} \delta \mathbf{t}_s \otimes \mathbf{X} \\ \frac{1}{|\Omega_f|} \int_{\Gamma} \delta \mathbf{t}_f \otimes \mathbf{X} \end{Bmatrix} = \begin{Bmatrix} \frac{1}{|\Omega_s|} \sum_{i=1}^4 \delta \mathbf{f}_s \otimes \mathbf{X}^{(i)} \\ \frac{1}{|\Omega_f|} \sum_{i=1}^4 \delta \mathbf{f}_p \otimes \mathbf{X}^{(i)} \end{Bmatrix}$$

which, in lieu of (10) can be written as

$$\begin{Bmatrix} \delta \mathbf{P}_{sM} \\ \delta \mathbf{P}_{fM} \end{Bmatrix} = \begin{Bmatrix} \frac{1}{|\Omega_s|} \sum_{i=1}^4 \sum_{j=1}^4 (\mathbf{K}_{uu_{ij}} \delta \mathbf{u}^{(j)} + \mathbf{K}_{up_{ij}} \delta p^{(j)}) \otimes \mathbf{X}^{(i)} \\ \frac{1}{|\Omega_f|} \sum_{i=1}^4 \sum_{j=1}^4 (\mathbf{K}_{pu_{ij}} \delta \mathbf{u}^{(j)} + \mathbf{K}_{pp_{ij}} \delta p^{(j)}) \otimes \mathbf{X}^{(i)} \end{Bmatrix}$$

We then substitute $\delta \mathbf{u}^{(j)} = \delta \mathbf{F}_M \mathbf{X}^{(j)}$ and $\delta p^{(j)} = \delta \tilde{p}|_c + \delta(\nabla_X \tilde{p})|_c \cdot (\mathbf{X}^{(j)} - \mathbf{X}_c)$ in the above and compare with (11)

$$\begin{Bmatrix} \delta \mathbf{P}_{sM} \\ \delta \mathbf{P}_{fM} \end{Bmatrix} = \mathbf{K}_M \begin{Bmatrix} \delta \mathbf{F}_M \\ \delta \tilde{p} \end{Bmatrix} \quad (11)$$

to obtain macroscopic tangent stiffness \mathbf{K}_M

Algorithm 2 Fluid filled porous solid case

```

FM ← I                                     ▷ Initialize deformation gradient
for  $E \in \mathcal{T}_h$  do                               ▷ loop over macroscale finite elements
    for  $g \in \mathcal{G}$  do                                 ▷ loop over gauss points
        RVE ↔  $g$                                      ▷ Assign a RVE to each gauss point
        Discretize the RVE
        Calculate homogenized macroscopic tangent stiffness and store it
    Assemble macroscopic tangent stiffness over gauss points
Assemble macroscopic tangent stiffness over finite elements
while  $t \leq T$  do
    Apply increment of macro load
    while (Internal force-Macro load > TOL) do
        Solve macroscale problem for  $\delta \mathbf{F}_M$ 
        FM ← FM +  $\delta \mathbf{F}_M$                                ▷ Update deformation gradient
        for  $E \in \mathcal{T}_h$  do                               ▷ loop over macroscale finite elements
            for  $g \in \mathcal{G}$  do                                 ▷ loop over gauss points
                Prescribe periodic BCs
                Solve RVE problem
                Calculate first P-K stress
            Compute internal forces at finite element nodes
    
```

4 Conclusions and outlook

We combined the features of two techniques in literature to design an algorithm for numerical homogenization of fluid filled porous solids. For the clarity of explanation, we first presented the algorithm for the pure mechanical case in which the entire microstructure is a solid phase. We then proceeded to explain the algorithm for the case in which the microstructure has both solid and fluid phases. The details of the derivation of the RVE level system of equations will be dealt with in part-II of this paper.

References

- [1] Z. Hashin and S. Shtrikman. On some variational principles in anisotropic and nonhomogeneous elasticity. *Journal of the Mechanics and Physics of Solids*, 10(4):335–342, 1962.
- [2] R. Hill. Elastic properties of reinforced solids: Some theoretical principles. *Journal of the Mechanics and Physics of Solids*, 11(5):357–372, 1963.
- [3] R. Hill. A self-consistent mechanics of composite materials. *Journal of the Mechanics and Physics of Solids*, 13(4):213–222, 1965.
- [4] R. Hill. On constitutive macro-variables for heterogeneous solids at finite strain. *Proceedings Mathematical Physical and Engineering Sciences*, 326(1565):131–147, 1972.
- [5] Z. Hashin. Analysis of composite materials—a survey. *Journal of Applied Mechanics*, 50(3):481–505, 1983.
- [6] T. I. Zohdi and P. Wriggers. *Introduction to computational micromechanics*. Springer Science and Business Media, 2008.
- [7] K. Terada and N. Kikuchi. A class of general algorithms for multi-scale analyses of heterogeneous media. *Computer Methods in Applied Mechanics and Engineering*, 190:5427–5464, 2001.
- [8] J. Fish. *Practical multiscaleing*. John Wiley and Sons Inc, 1 edition, 2014.
- [9] C. Sandström, F. Larsson, and K. Runesson. Homogenization of coupled flow and deformation in a porous material. *Computer Methods in Applied Mechanics and Engineering*, 308:535–551, 2016.
- [10] M.G.D. Geers, V.G. Kouznetsova, and W.A.M. Brekelmans. Multi-scale computational homogenization: Trends and challenges. *Journal of Computational and Applied Mathematics*, 234(7):2175 – 2182, 2010. Fourth International Conference on Advanced Computational Methods in Engineering (ACOMEN 2008).
- [11] I. Ozdemir, W. A. M. Brekelmans, and M. G. D. Geers. Fe2 computational homogenization for the thermo-mechanical analysis of heterogeneous solids. *Computer Methods in Applied Mechanics and Engineering*, 198(3):602 – 613, 2008.
- [12] Jörg Schröder. A numerical two-scale homogenization scheme: the fe2-method. In *Plasticity and beyond*, pages 1–64. Springer, 2014.
- [13] S. Hazanov. Hill condition and overall properties of composites. *Archive of Applied Mechanics*, 68(6):385–394, 1998.
- [14] S. Hazanov. On apparent properties of nonlinear heterogeneous bodies smaller than the representative volume. *Acta Mechanica*, 134(3-4):123–134, 1999.
- [15] M. Hori and S. Nemat-Nasser. On two micromechanics theories for determining micro-macro relations in heterogeneous solids. *Mechanics of Materials*, 31(10):667–682, 1999.
- [16] Z. Yuan and J. Fish. Toward realization of computational homogenization in practice. *International Journal for Numerical Methods in Engineering*, 73(3):361–380, 2008.
- [17] I. Temizer and P. Wriggers. Homogenization in finite thermoelasticity. *Journal of the Mechanics and Physics of Solids*, 59(2):344 – 372, 2011.
- [18] D. Perić, E. A. de Souza Neto, R. A. Feijóo, M. Partovi, and A. J. Carneiro Molina. On micro-to-macro transitions for multi-scale analysis of non-linear heterogeneous materials: unified variational basis and finite element implementation. *International Journal for Numerical Methods in Engineering*, 87(1-5):149–170, 2011.
- [19] F. Larsson and K. Runesson. On two-scale adaptive fe analysis of micro-heterogeneous media with seamless scale-bridging. *Computer Methods in Applied Mechanics and Engineering*, 200:2662–2674, 2011.
- [20] S. Saeb, P. Steinmann, and A. Javili. Aspects of computational homogenization at finite deformations: A unifying review from reuss’ to voigt’s bound. *Applied Mechanics Reviews*, 68(5):050801–1–050801–33, 2016.
- [21] C. C. Swan. Techniques for stress- and strain-controlled homogenization of inelastic periodic composites. *Computer Methods in Applied Mechanics and Engineering*, 117:249–267, 1994.
- [22] J. C. Michel, H. Moulinec, and P. Suquet. Effective properties of composite materials with periodic microstructure: a computational approach. *Computer Methods in Applied Mechanics and Engineering*, 172:109–143, 1999.

- [23] N. Takano, M. Zako, and M. Ishizono. Multi-scale computational method for elastic bodies with global and local heterogeneity. *Scientific Modeling and Simulation SMNS*, 7(2):111–132, 2000.
- [24] V. V. Kouznetsova, W. A. M. Brekelmans, and F. P. T. Baaijens. An approach to micro-macro modeling of heterogeneous materials. *Computational Mechanics*, 27(1):37–48, 2001.
- [25] C. Miehe and A. Koch. Computational micro-to-macro transitions of discretized microstructures undergoing small strains. *Archive of Applied Mechanics*, 72, 2002.
- [26] C. Miehe. Strain-driven homogenization of inelastic microstructures and composites based on an incremental variational formulation. *International Journal for Numerical Methods in Engineering*, 55(11):1285–1322, 2002.
- [27] C. Miehe. Computational micro-to-macro transitions for discretized micro-structures of heterogeneous materials at finite strains based on the minimization of averaged incremental energy. *Computer Methods in Applied Mechanics and Engineering*, 192:559–591, 2003.
- [28] I. Temizer and T. I. Zohdi. A numerical method for homogenization in non-linear elasticity. *Computational Mechanics*, 40(2):281–298, 07 2007.
- [29] I. Temizer; P. Wriggers. On the computation of the macroscopic tangent for multiscale volumetric homogenization problems. *Computer Methods in Applied Mechanics and Engineering*, 198:495–510, 2008.
- [30] I. Temizer and P. Wriggers. An adaptive multiscale resolution strategy for the finite deformation analysis of microheterogeneous structures. *Computer Methods in Applied Mechanics and Engineering*, 200:2639–2661, 2011.
- [31] F. Larsson, K. Runesson, S. Saroukhani, and R. Vafadari. Computational homogenization based on a weak format of micro-periodicity for rve-problems. *Computer Methods in Applied Mechanics and Engineering*, 200:11–26, 2011.
- [32] A. Sengupta, P. Papadopoulos, and R. L. Taylor. A multiscale finite element method for modeling fully coupled thermomechanical problems in solids. *International Journal for Numerical Methods in Engineering*, 91(13):1386–1405, 2012.
- [33] N. P. van Dijk. Formulation and implementation of stress- and/or strain-driven computational homogenization for finite strain. *International Journal for Numerical Methods in Engineering*, pages 1009–1028, 2015.
- [34] Eduardo A de Souza Neto, Raúl A Feijóo, and AA Novotny. Variational foundations of large strain multiscale solid constitutive models: kinematical formulation. *Advanced computational materials modeling: from classical to multi-scale techniques-scale techniques*, 2011.
- [35] Saumik Dana, Benjamin Ganis, and Mary F. Wheeler. A multiscale fixed stress split iterative scheme for coupled flow and poromechanics in deep subsurface reservoirs. *Journal of Computational Physics*, 352:1–22, 2018.
- [36] Saumik Dana and Mary F Wheeler. Design of convergence criterion for fixed stress split iterative scheme for small strain anisotropic poroelastoplasticity coupled with single phase flow. *arXiv preprint arXiv:1912.06476*, 2019.
- [37] Saumik Dana. System of equations and staggered solution algorithm for immiscible two-phase flow coupled with linear poromechanics. *arXiv preprint arXiv:1912.04703*, 2019.
- [38] Saumik Dana, Joel Ita, and Mary F Wheeler. The correspondence between voigt and reuss bounds and the decoupling constraint in a two-grid staggered algorithm for consolidation in heterogeneous porous media. *Multiscale Modeling & Simulation*, 18(1):221–239, 2020.
- [39] Saumik Dana, Xiaoxi Zhao, and Birendra Jha. Two-grid method on unstructured tetrahedra: Applying computational geometry to staggered solution of coupled flow and mechanics problems. *arXiv preprint arXiv:2102.04455*, 2021.
- [40] S. Dana and M. F. Wheeler. Convergence analysis of fixed stress split iterative scheme for anisotropic poroelasticity with tensor biot parameter. *Computational Geosciences*, 22(5):1219–1230, 2018.
- [41] S. Dana and M. F. Wheeler. Convergence analysis of two-grid fixed stress split iterative scheme for coupled flow and deformation in heterogeneous poroelastic media. *Computer Methods in Applied Mechanics and Engineering*, 341:788–806, 2018.
- [42] S. Dana. *Addressing challenges in modeling of coupled flow and poromechanics in deep subsurface reservoirs*. PhD thesis, The University of Texas at Austin, 2018.